applied sciences

MDPI

Article

Fast-Tunable Terahertz Metamaterial Absorber Based on Polymer Network Liquid Crystal

Zhiping Yin [1], Chaofan Wan [1], Guangsheng Deng [1,*], Andong Zheng [1], Peng Wang [1], Yang Yang [1], Sheng Gao [1], Jun Yang [1], Fei Cai [1], Zelun Li [2] and Hongbo Lu [1,*]

[1] National Key Laboratory of Advanced Display Technology, Academy of Photoelectric Technology, Hefei University of Technology, Hefei 230009, China; zpyin@hfut.edu.cn (Z.Y.); 18715279964@163.com (C.W.); 18656098638@163.com (A.Z.); wpvilf@126.com (P.W.); yangyang19@mail.hfut.edu.cn (Y.Y.); gao1sheng001@outlook.com (S.G.); junyang@hfut.edu.cn (J.Y.); flycai@gmail.com (F.C.)

[2] College of Mechanical and Power Engineering, Chongqing University of Science and Technology, Chongqing 401331, China; zelunli@cqust.edu.cn

* Correspondence: dgsh@hfut.edu.cn (G.D.); bozhilu@hfut.edu.cn (H.L.)

Received: 18 October 2018; Accepted: 21 November 2018; Published: 1 December 2018

Abstract: This paper introduces a tunable metamaterial absorber (MA) based on polymer network liquid crystal (PNLC) in the terahertz (THz) frequency band. Under the optimal polymerization condition, through electrical control of the orientation of the PNLC embedded in the frequency selective surface, the resonant frequency of the absorber can be tuned from 416.5 to 405.0 GHz, corresponding to fractional frequency bandwidth of 2.8%. The experimental results show that the proposed MA based on the PNLC offers an adjustment time of 10 ms and recovery time of 85 ms, which is significantly faster than the tunable metamaterial devices based on conventional nematic liquid crystal (LC).

Keywords: polymer network; absorber; liquid crystal; response time; terahertz

1. Introduction

Over the past few years, realization of telecommunication, imaging, sensing, and biomedical instruments and devices in the THz regime of the electromagnetic spectrum have attracted a great deal of research attention. This is due to the prominent potential of the THz frequency regime in the realization of highly efficient and ultra-broadband wireless communication systems [1–3]. A variety of THz devices have been recently emerged, in which the THz absorbers exert an important role in the THz systems, including the sensors, detectors and imaging instruments [4,5].

Metamaterials are widely known due to their unique physical properties not readily observed in natural materials [6]. They are artificially composited to affect the energy of the electromagnetic radiation to achieve abnormal properties such as negative permittivity and negative permeability [7,8]. Ever since Landy et al. presented the design for an absorbing metamaterial with near unity absorbance in 2008 [9], the metamaterial absorbers (MAs) have attracted an extensive research attention. Afterwards, various MAs were designed to fulfill different demands. Zhu et al. demonstrated an ultra-broadband, polarization-insensitive, and wide-angle MA for THz regime [10]. Shen et al. fabricated a MA that had three distinctive absorption peaks at 0.5, 1.03, and 1.71 THz with absorption rates of 96.4%, 96.3%, and 96.7%, respectively [11]. However, most of them could only operate at a single frequency or in a limited range of frequencies. To overcome this issue, the tunable absorbers were presented by researchers [12,13]. Shrekenhamer et al. put forward the electronically-tunable MA by incorporation of LC into strategic locations within the metamaterial unit cell [14]. Then, various tunable

MAs based on LC, such as single-band MA [6], triple-band MA [15], and polarization-dependent MA [16], have been reported.

LC, as a tunable material, is generally known that the rotation of the nematic LC embedded in the absorber can be guided by the bias voltage, resulting in the shift of the resonant frequency [17]. However, the response time of the LC-based devices is quite slow, which hinders their potential applications. The response time of the nematic LC depends on several factors, such as the cell gap, viscoelastic coefficient, and applied voltage [18]. The rotation time can be greatly cut down by applying a large bias voltage. However, the recovery time after removing the bias voltage may be diminished by the larger restoring elastic torque. Then, the free recovery time may be reduced by introducing the polymer network liquid crystal (PNLC) [19].

In this paper, we present a tunable MA based on the PNLC in terahertz band. Compared to the previously reported LC-based Mas, the metal ground plane is replaced by a transparent indium-tin-oxide (ITO) film so that the UV light can be transmitted through the ground electrode plate to polymerize the internal network. The experimental results show that the PNLC-based MA not only provides wideband tunability but also greatly accelerates the response time.

2. Structure Design and Absorption Mechanisms

The design of the MA begins with the frequency selective surface (FSS), which is a two-dimensional periodic metal patch array on the dielectric surface and exhibits obvious band-pass or band-stop filtering characteristics when interacting with electromagnetic waves. The common basic units of FSS are dipoles, crosses, square rings, etc. In this paper, the circular patch array is adopted and fabricated by lithography and etching. Figure 1 shows the fabricated patch array.

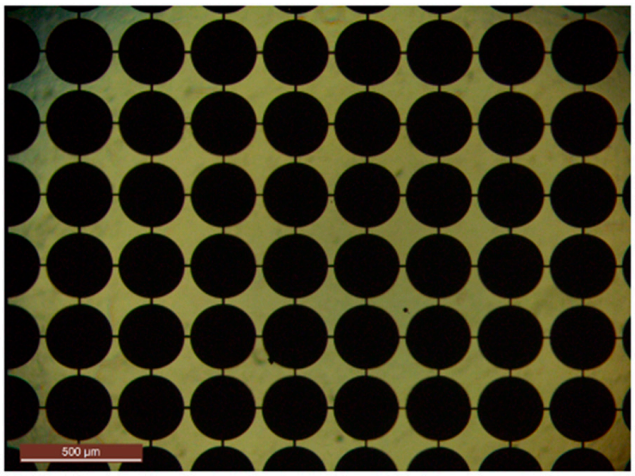

Figure 1. Fabricated patch array.

The PNLC (also known as anisotropic LC gel) has been extensively studied in the field of electrically tuned scattering devices [20]. In this paper, the mass ratio of 95% LC host SLC103014-200 (S200) (Shi jiazhuang Chenzhi Yonghua Display Material Co., Ltd., Shi jiazhuang, China) is first mixed with a mass ratio of 5% photoreactive difunctional monomer RM257 (Jiangsu Hecheng Advanced Materials Co., Ltd., Nanjing, China) and a small amount of photoinitiator Benzoin Methyl Ether (TOKYO CHEMICAL INDUSTRY CO., LTD., Tokyo, Japan). Then, the photopolymerization precursor is filled into the LC cell. After this, a UV curing process is performed to induce the crosslinking of the polymer network [21]. Figure 2 sketches a schematic diagram of the PNLC manufacturing process.

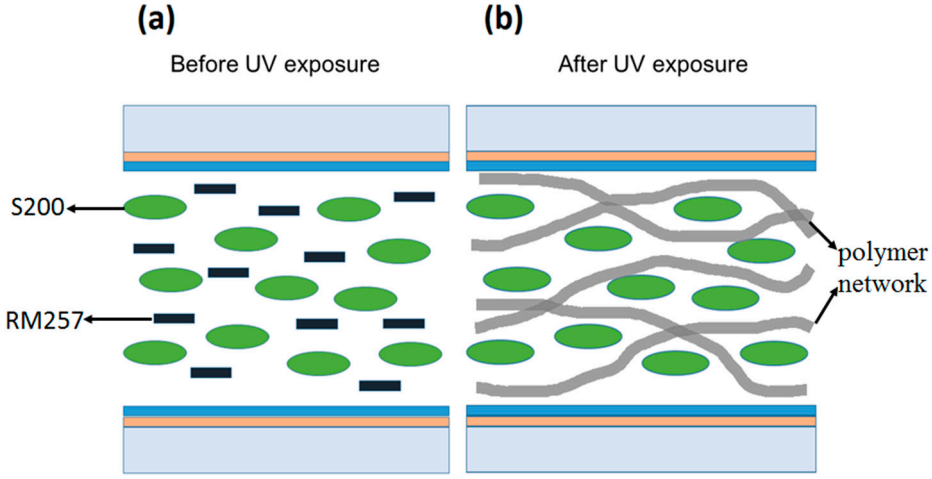

Figure 2. (**a**) Mixture of the liquid crystal (LC) host and photopolymer sable monomer filled into a LC cell. (**b**) The form of the polymer network after the UV exposure.

Figure 3 presents the structure of the PNLC-based MA. This device is composed of a patterned copper layer (FSS) and an ITO layer spaced apart by PNLC. The top copper layer is geometrically patterned in order to strongly couple to a uniform incident electric field and serves as a top electrode. By pairing the top layer with an ITO plane, it serves not only as a bottom electrode but also as a metal ground. Besides, the inner surfaces of the copper layer and the ITO layer are coated by the polyimide (PI) alignment layers to leave the orientation of the LC molecules parallel to the surface of the electrode without the bias voltage. When the driving voltage is applied, the alignment of the liquid crystal molecules is parallel to the excitation electric field.

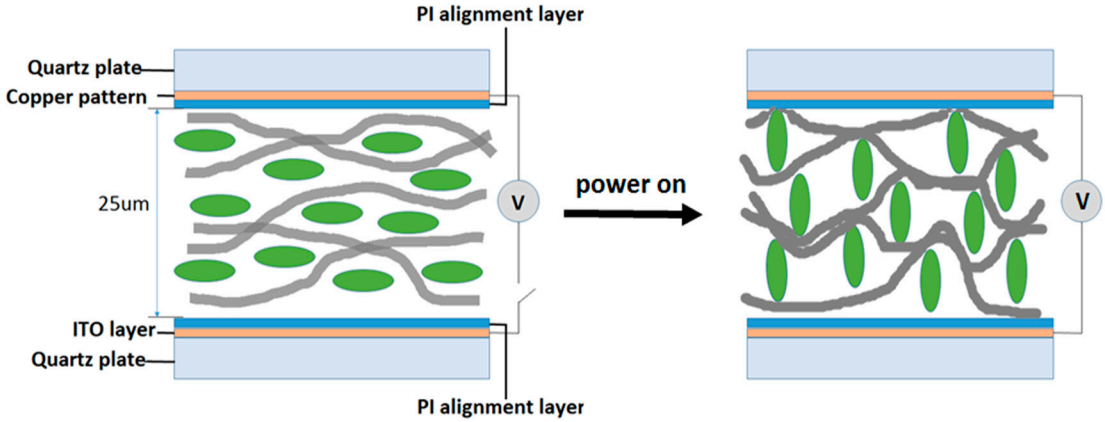

Figure 3. Schematic diagram of the polymer network liquid crystal (PNLC)-based metamaterial absorber (MA).

The resonant structure may be considered as a circular patch, with high aspect ratios. According to the antenna theory, the resonant mode within the structure is a cavity mode [22]. The orientation of the LC molecules may be redirected by an external electrical field excited by a bias voltage between the top metal pattern layer and the ITO ground. As a result, the permittivity of the LC layer continuously varies with the change of the bias voltage. Specially, when the LC molecules turn to the direction perpendicular to the surface of the electrode, permittivity reaches its peak value with the saturation state. Therefore, the LC permittivity may be electronically controlled between these two states. The resonant frequency of a MA depends on the dielectric permittivity of the LC layer so that it may be shifted by changing the bias voltage.

3. Experimental Results and Comparative Analysis

Figure 4 shows the fabricated prototype, with the glass substrate size of 2 cm × 2 cm and 60 × 50 unit cells with the dimensions of a = 300 μm, b = 15 μm, and r = 140 μm. A total of five sets of experiments were carried out, in which the nematic LC (S200)-based MA was used as the contrast experiment, representing the common LC-based THz devices. In addition, the PNLC-based MAs were used as exploratory experiments with different exposure time. The absorptivity of MAs can be determined by $A = 1 - |s_{11}|^2 - |s_{21}|^2$, where A, s_{11}, and s_{21} denote the absorptivity, reflection coefficient, and transmission coefficient, respectively. Since the transmission coefficient is equal to zero due to the existence of the ITO plate, the absorptivity can be simplified as $A = 1 - |s_{11}|^2$.

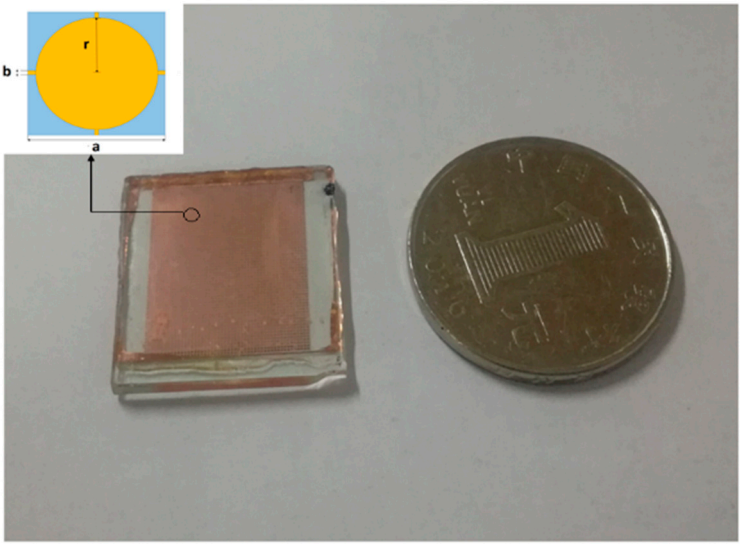

Figure 4. Fabricated metamaterial absorber.

The absorption spectra of the S200 LC-based MA is shown in Figure 5. It was observed that the peak resonant frequency occurs at 411.0 GHz without the bias voltage (0 V). With the increase of the driving voltage, the absorption peak frequency shows a red shift until it reaches a saturated bias voltage of 5 V. The resonance peak frequency under fully biased voltage is 393.5 GHz

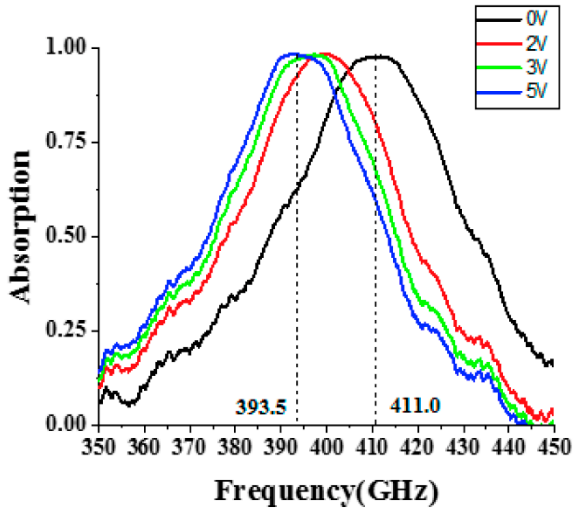

Figure 5. Measured absorption spectra of the S200 LC-based MA.

Then, in Figure 6a–d, the tunabilities of the PNLC-based MAs in the case of UV exposure times of 0 min, 30 min, 60 min and 90 min, were experimentally demonstrated, and the resonant frequencies were found to be 406.5 GHz, 416.5 GHz, 416.5 GHz, and 418.5 GHz, respectively, with a bias voltage of 0 V. For each case, by increasing the bias voltage, the absorption peaks continuously shift to lower frequencies until the LC molecules were fully rotated. As a result, the resonant frequencies were located at 391.5 GHz, 402.5 GHz, 405.0 GHz, and 407.5 GHz, respectively, under the saturated bias voltage.

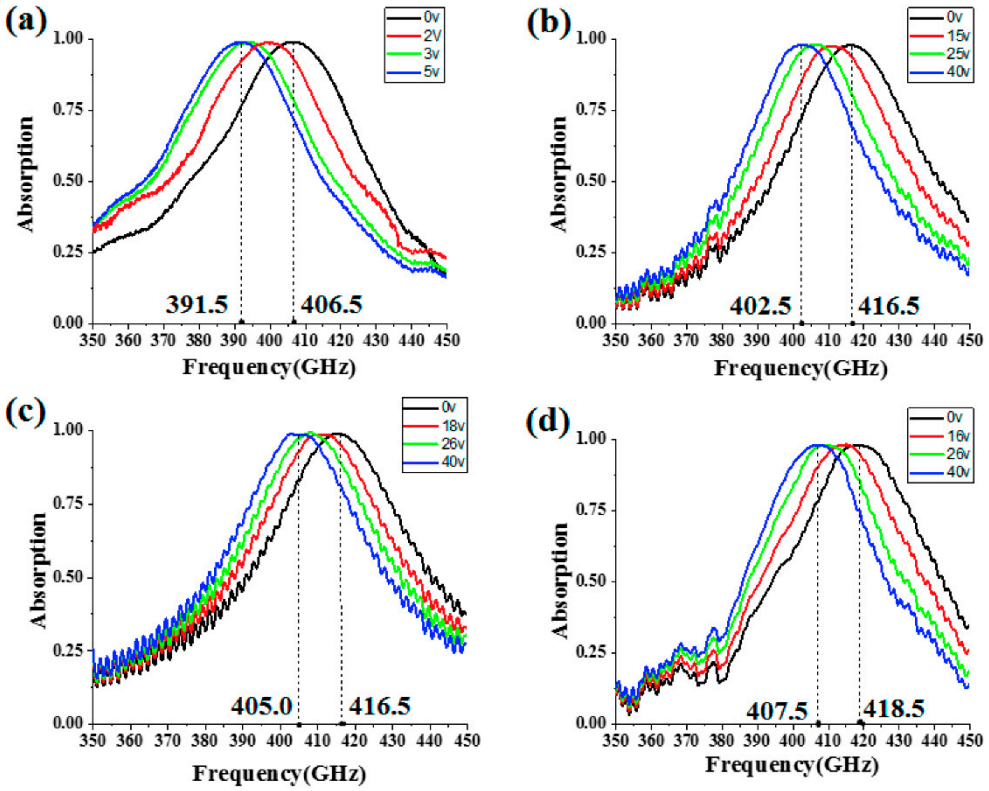

Figure 6. Measured absorption spectra of the PNLC based MA: (**a**) Without UV exposure; (**b**) with 30 min UV exposure; (**c**) with 60 min UV exposure; and (**d**) with 90 min UV exposure.

From Figure 6, it can be seen that for PNLC-based MA, the saturated bias voltage (40 V) after UV exposure is much higher than that (5 V) of the initial state. This may be attributed to the strong anchoring of the polymer network after UV exposure as the LC molecules in the polymer network require a greater voltage to spin. Moreover, with the increase of UV exposure time, the peak absorption frequency in both the unbiased state and fully biased state shows a slightly blue shift. Hence, increasing UV exposure time leads to a decrease of the effective permittivity of the PNLC.

The measured results have proved the tunability of the absorption peak of the designed MAs. In practical applications, it is required that the absorption peak of the MAs can be quickly converted under the driving voltage. As can be seen from the foregoing, the LC is treated as the tunable electromagnetic material. Under the action of driving voltage, the molecular orientation changes, leading to the change of dielectric constant so that the MAs are capable of tunable resonant frequency in THz band. According to the electro-optic effect of the LC, under the driving of voltage, the reorientation of LC molecules causes the optical axis to rotate so that the transmission intensity correspondingly changes. So, we set up the experimental platform as shown in the Figure 7. The sample was placed between polarizers whose polarization direction was perpendicular to each other. At this time, the angle between the transmission axis of the sample and the transmission axis of the two polarizers was 45°, and the light source could pass through. When the driving voltage was applied to the sample, the LC molecules rotated and kept parallel to the electric field. The sample could not polarize the

incident light source, in this case, the light source could not pass through the polarizers perpendicular to each other. Therefore, the response speed of the absorption peak is reflected by detecting the intensity of the transmitted light during power-on and power-off. It should be noticed that we measured the response speed here at visible frequencies instead of THz frequencies. Because the polarization state of transmitted light, which is affected by birefringence effect of liquid crystal at visible frequencies, is determined by molecular rotation of LC. However, the LC molecular rotation is also responsible for the change of permittivity of LC layer in terahertz band. As the rotation speed of LC molecules is mainly determined by driving voltages, it is independent on testing frequencies.

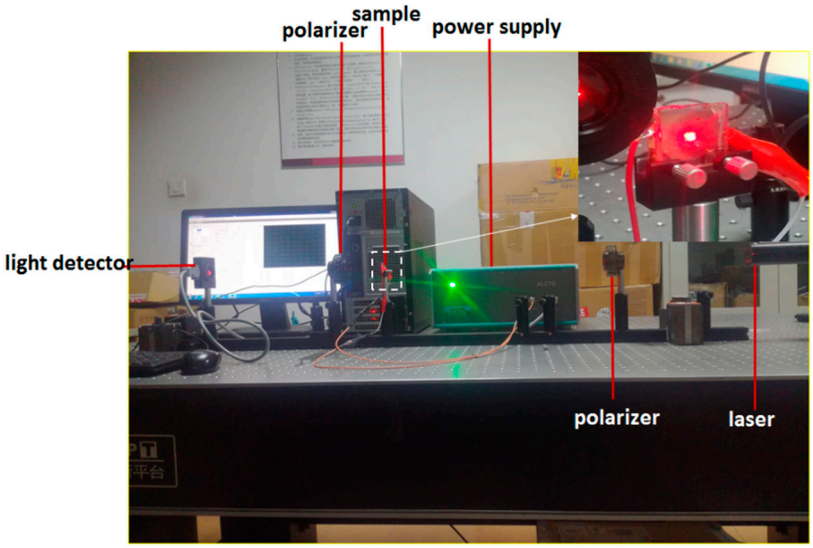

Figure 7. Experimental platform for measuring the response time of the MAs.

Taking the nematic S200-based absorbor as an example, the experimental results show that the absorption peak of the sample is at 411.0 GHz when no voltage is applied. Correspondingly, the detected light intensity is the strongest. When a saturated voltage is applied, the absorption peak of the sample is at 393.5 GHz and the detected light intensity is the weakest. Therefore, the time required for the relative light intensity of the transmitted light from 90% to 10% is defined as the adjustment time of the absorber. And the time consumed for the relative light intensity from 10% to 90% is defined as the recovery time of the absorber when the power is off [23]. The adjustment time and recovery time comprehensively reflect the response speed of the absorber to the driving voltage. The measured results of response time of the LCand the PNLC-based MAs are illustrated in Figure 8.

From Figure 8a, it is clear that the adjustment time and recovery time of the nematic S200 LC-based MA are 47.5 ms and 1466.0 ms, respectively. However, as shown in Figure 8b, after the UV photopolymerization of the PNLC for 30 min, the response time drastically reduces to 7.5 ms and 206.9 ms by an order of magnitude. This is due to the strong anchoring of the polymer network, corresponding to a larger splay elasticity, as the free relaxation time of the liquid crystal molecules becomes much shorter.

Furthermore, Table 1 lists the response time of various samples. By increasing the UV exposure time from 30 min to 90 min, the recovery time of the MA can be further decreased from 207.0 ms to 84.0 ms. This is due to the fact that for a shorter exposure time, the formed polymer network is sparser, and the less liquid crystals are limited by the network, corresponding to a smaller elastic coefficient. With the increase of the exposure time, the polymer network will be denser in the sample, so the anchoring effect of the network on the liquid crystal will also increase, which corresponds to a larger elastic coefficient. However, there is no obviously change of the response time when the UV exposure time increases from 60 min to 90 min, which indicates that the photopolymerization precursor of the polymer network has been thoroughly reacted by the UV light.

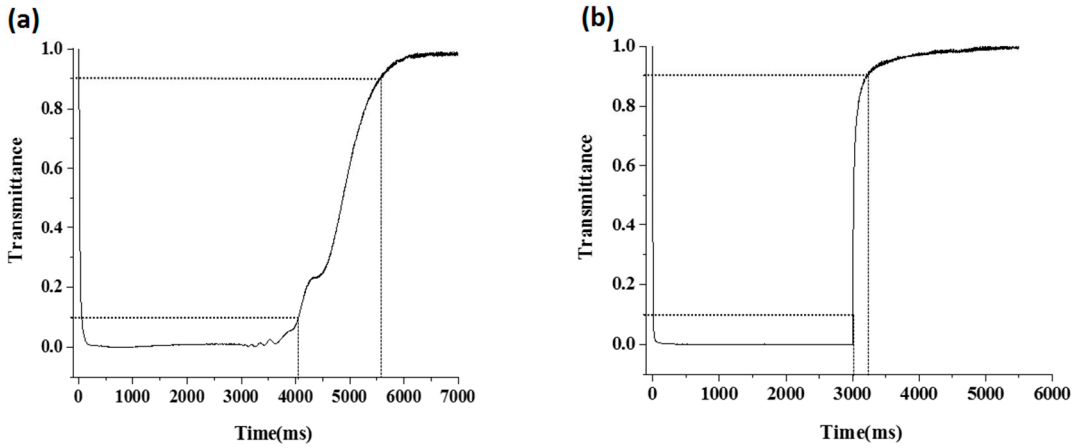

Figure 8. Curves of measured response time of the MAs: (**a**) The MA based on the nematic LC (S200) and (**b**) the MA based on the PNLC with 30 min UV exposure time.

Table 1. Results of measured response time of MAs.

MAs	Adjustment Time (ms)	Recovery Time (ms)
nematic LC (S200)	47.5	1466.0
PNLC (0 min)	51.5	2346.0
PNLC (30 min)	7.5	207.0
PNLC (60 min)	10.0	85.0
PNLC (90 min)	8.0	84.0

4. Conclusions

A tunable MA based on the polymer network liquid crystal is presented in this paper. Compared with the conventional tunable nematic LC-based absorbers, the PNLC-based absorber offers a faster response speed. In addition, by increasing the exposure time of the PNLC, the response time may be further reduced until the photopolymerization precursor is completely reacted. The proposed structure is expected to find many applications in tunable THz devices such as fast-response phase shifters and sensors.

Author Contributions: G.D. and H.L. conceived and designed the experiments; A.Z., P.W., Y.Y. and S.G. performed the experiments; J.Y. analyzed the data; Z.Y. and C.W. wrote the original draft; F.C. and Z.L. reviewed manuscript.

Funding: This research was funded by National Natural Science Foundation of China (Grant No. 61871171, 51607050) and Chongqing Research Program of Basic Research and Frontier Technology (Grant No. cstc2018jcyjAX0291).

Conflicts of Interest: The authors declare no conflict of interest.

References

1. Chen, H.T.; Padilla, W.J.; Zide, J.M.; Gossard, A.C.; Taylor, A.J.; Averitt, R.D. Active terahertz metamaterial devices. *Nature* **2006**, *444*, 597–600. [CrossRef] [PubMed]
2. Akyildiz, I.F.; Han, C.; Nie, S. Combating the Distance Problem in the Millimeter Wave and Terahertz Frequency Bands. *IEEE Commun. Mag.* **2018**, *56*, 102–108. [CrossRef]
3. Nasr, M.; Richard, J.T.; Skirlo, S.A.; Heimbeck, M.S.; Joannopoulos, J.D.; Soljacic, M.; Everitt, H.O.; Domash, L. Narrowband Metamaterial Absorber for Terahertz Secure Labeling. *J. Infrared Millim. Terahertz Waves* **2017**, *38*, 1120–1129. [CrossRef]
4. Yahiaoui, R.; Guillet, J.P.; de Miollis, F.; Mounaix, P. Ultra-flexible multiband terahertz metamaterial absorber for conformal geometry applications. *Opt. Lett.* **2013**, *38*, 4988–4990. [CrossRef]
5. Khatib, M.; Perenzoni, M. A Low-Noise Direct Incremental A/D Converter for FET-Based THz Imaging Detectors. *Sensors* **2018**, *18*, 1867. [CrossRef] [PubMed]

6. Deng, G.; Xia, T.; Jing, S.; Yang, J.; Lu, H.; Yin, Z. A Tunable Metamaterial Absorber Based on Liquid Crystal Intended for F Frequency Band. *IEEE Antennas Wirel. Propag. Lett.* **2017**, *16*, 2062–2065. [CrossRef]
7. Gnawali, R.; Banerjee, P.P.; Haus, J.W.; Reshetnyak, V.; Evans, D.R. Optical propagation through anisotropic metamaterials: Application to metallo-dielectric stacks. *Opt. Commun.* **2018**, *425*, 71–79. [CrossRef]
8. Bakir, M.; Karaaslan, M.; Akgol, O.; Altintas, O.; Unal, E.; Sabah, C. Sensory applications of resonator based metamaterial absorber. *Optik* **2018**, *168*, 741–746. [CrossRef]
9. Landy, N.I.; Sajuyigbe, S.J.; Mock, J.; Smith, D.R.; Padilla, W.J. Perfect metamaterial absorber. *Phys. Rev. Lett.* **2008**, *100*, 207402. [CrossRef] [PubMed]
10. Zhu, J.; Ma, Z.; Sun, W.; Ding, F.; He, Q.; Zhou, L.; Ma, Y. Ultra-broadband terahertz metamaterial absorber. *Appl. Phys. Lett.* **2014**, *105*, 021102. [CrossRef]
11. Shen, X.; Yang, Y.; Zang, Y.; Gu, J.; Han, J.; Zhang, W.; Cui, T. Triple-band terahertz metamaterial absorber: Design, experiment, and physical interpretation. *Appl. Phys. Lett.* **2012**, *101*, 154102. [CrossRef]
12. Andryieuski, A.; Lavrinenko, A.V. Graphene metamaterials based tunable terahertz absorber: Effective surface conductivity approach. *Opt. Express* **2013**, *21*, 9144–9155. [CrossRef] [PubMed]
13. Zhang, C.; Hu, X. Three-Dimensional Single-Port Labyrinthine Acoustic Metamaterial: Perfect Absorption with Large Bandwidth and Tunability. *Phys. Rev. Appl.* **2016**, *6*, 064025. [CrossRef]
14. Shrekenhamer, D.; Chen, W.C.; Padilla, W.J. Liquid crystal tunable metamaterial absorber. *Phys. Rev. Lett.* **2013**, *110*, 177403. [CrossRef] [PubMed]
15. Wang, R.; Li, L.; Liu, J.; Yan, F.; Tian, F.; Tian, H.; Zhang, J.; Sun, W. Triple-band tunable perfect terahertz metamaterial absorber with liquid crystal. *Opt. Express* **2017**, *25*, 32280–32289. [CrossRef]
16. Deng, G.; Lu, Y.; Yin, Z.; Lai, W.; Lu, H.; Yang, J.; Yang, A.; Ye, Y.; Liu, D.; Chi, B. A Tunable Polarization-Dependent Terahertz Metamaterial Absorber Based on Liquid Crystal. *Electronics* **2018**, *7*, 27. [CrossRef]
17. Altmann, K.; Reuter, M.; Garbat, K.; Koch, M.; Dabrowski, R.; Dierking, I. Polymer stabilized liquid crystal phase shifter for terahertz waves. *Opt. Express* **2013**, *21*, 12395–12400. [CrossRef]
18. Sun, J.; Wu, S.T. Recent advances in polymer network liquid crystal spatial light modulators. *J. Polym. Sci. Part B Polym. Phys.* **2014**, *52*, 183–192. [CrossRef]
19. White, T.J.; Broer, D.J. Programmable and adaptive mechanics with liquid crystal polymer networks and elastomers. *Nat. Mater.* **2015**, *14*, 1087–1098. [CrossRef]
20. Fan, Y.H.; Lin, Y.H.; Ren, H.; Gauza, S.; Wu, S.T. Fast-response and scattering-free polymer network liquid crystals for infrared light modulators. *Appl. Phys. Lett.* **2004**, *84*, 1233–1235. [CrossRef]
21. Bi, S.; Peng, H.; Long, S.; Ni, M.; Liao, Y.; Yang, Y.; Xue, Z.; Xie, X. High modulus and low-voltage driving nematic liquid-crystalline physical gels for light-scattering displays. *Soft Matter* **2013**, *9*, 7718–7725. [CrossRef]
22. Nam, S.; Lee, B.; Kwak, C.; Lee, J. A New Class of K-Band High-Q Frequency-Tunable Circular Cavity Filter. *IEEE Trans. Microw. Theory Tech.* **2018**, *66*, 1228–1237. [CrossRef]
23. Chen, K.M.; Gauza, S.; Xianyu, H.; Wu, S.T. Submillisecond Gray-Level Response Time of a Polymer-Stabilized Blue-Phase Liquid Crystal. *J. Disp. Technol.* **2010**, *6*, 49–51. [CrossRef]